chinaXiv:201703.00970v1

Transient Characteristics for Proton Gating in Laterally Coupled Indium−Zinc-Oxide Transistors

Ning Liu, Li Qiang Zhu,* Hui Xiao, Chang Jin Wan, Yang Hui Liu, and Jin Yu Chao

Ningbo Institute of Materials Technology and Engineering, Chinese Academy of Sciences, Ningbo 315201, People's Republic of China

ABSTRACT: The control and detection over processing, transport and delivery of chemical species is of great importance in sensors and biological systems. The transient characteristics of the migration of chemical species reflect the basic properties in the processings of chemical species. Here, we observed the field-configurable proton effects in a laterally coupled transistor gated by phosphorosilicate glass (PSG). The bias on the lateral gate would modulate the interplay between protons and electrons at the PSG/indium−zinc-oxide (IZO) channel interface. Due to the modulation of protons flux within the PSG films, the IZO channel current would be modified correspondingly. The characteristic time for the proton gating is estimated to be on the order of 20 ms. Such laterally coupled oxide based transistors with proton gating are promising for low-cost portable biosensors and neuromorphic system applications.

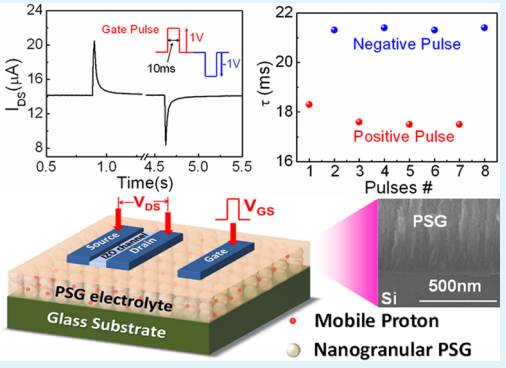

KEYWORDS: *proton gating, laterally coupling, interfacial electric-double layer (EDL), transient characteristics*

1. INTRODUCTION

In ion transistors, ions and charged molecules act as the charge carriers.[1−3] Due to the fact that such carriers carry specific chemical information and functionality, they can selectively regulate various functions and processes. Thus, ion transistor based circuits can be useful in delivering, regulating and establishing signaling patterns of ions and biomolecules.[4] Furthermore, ions, molecules or charged molecules could also be selectively transferred with the specific modified nanopores/nanochannels used in ion transistors.[5] In these nanofluids systems, the ionic/electronic coupling occurs in a way that the gate could control and monitor the ionic currents.[6,7] The ion migration could also be utilized to modulate the carrier transport characteristics of condensed materials greatly.[8] In ionic liquid or ionic gel electrolyte gated transistors, the movements of anions/cations in the electrolyte toward the positively/negatively charged electrode form an electric-double-layer (EDL), composed of a compact Helmholtz layer and a diffuse layer. As a result of the charge separation within a few angstroms, a high EDL capacitance above 1 μF/cm^2 could be obtained.[9−11] Therefore, field-induced electronic phase transitions and superconductivity are observed for specific condensed materials with transistor configuration.[8,12,13] In these devices, the gate bias triggers the migrations of ions within electrolyte, inducing the changes in carrier transport characteristics of condensed materials as a result.[14]

Recently, wide band-gap oxide semiconductors have been reported to be gated by solid state electrolytes, such as nanogranular SiO_2,[15−18] nanogranular Al_2O_3,[19] WO_x,[20,21] chitosan,[22−24] etc. Though the proton conductivities for these electrolytes have been discussed, the transient characteristics for proton gating still needed to be discussed in terms of characteristic time. On the other hand, the biological activities are always performed with ion signals, rather than the electrons.[25,26] Therefore, it is highly desirable to translate ionic signals into easily detectable electron signals. Thus, the realization of ionic/electronic coupled devices is meaningful for the interfacing between electrical signals and biological response in the biological systems. In this work, we observed the field-configurable proton effects in a laterally coupled transistor configuration. Due to the modulation of protons flux within the nanogranular phosphorosilicate glass (PSG) films, indium−zinc-oxide (IZO) channel current would be modified correspondingly. The transient characteristics of the proton gating were discussed, resulting in the extraction of characteristic time for proton gating. The laterally coupled oxide based transistors with proton gating are promising for low-cost portable biosensors and neuromorphic system applications.

2. EXPERIMENTAL PROCEDURE

Laterally coupled IZO transistors were fabricated on glass substrates at room temperature, as schematically shown in Figure 1. First, nanogranular phosphorosilicate glass (PSG) films were deposited on glass substrate and Si wafer at room temperature by plasma-enhanced chemical-vapor deposition (PECVD) using SiH_4 (94% SiH_4 + 6% PH_3) and O_2 as reactive gases. For characterizing the proton conductivities, the PSG film was also deposited on ITO glass substrate. Scanning electron microscopy (SEM) characterizations indicate the spongy microstructures for the as-deposited PSG films, as

Received: January 14, 2015
Accepted: March 5, 2015
Published: March 5, 2015

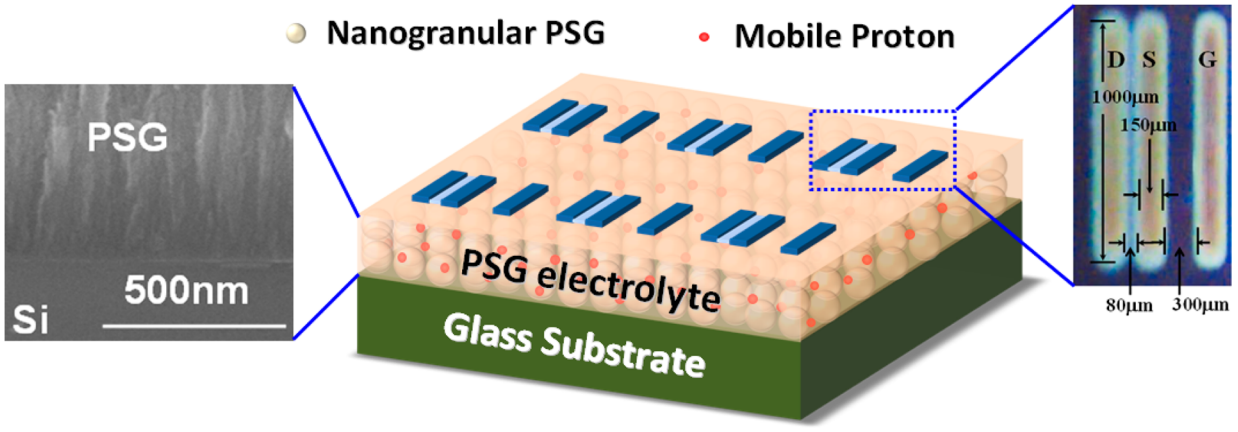

Figure 1. Schematic image of the IZO transistor arrays gated by PSG films with lateral gates. The left panel is the cross-sectional SEM image of as-deposited PSG films. The right panel is the optical image of laterally coupled IZO transistor.

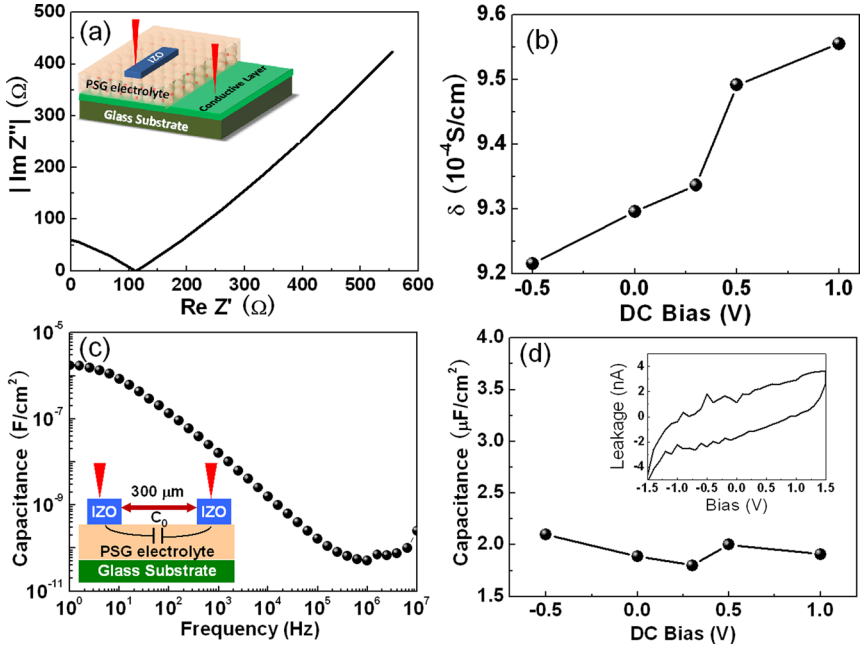

Figure 2. (a) Cole−Cole plots for the PSG film. Inset: the sample structure. (b) Proton conductivities (δ) as a function of DC bias during the measurements. (c) Frequency-dependent specific capacitance of the PSG film. Inset: the in-plane IZO/PSG/IZO sandwich structure. (d) Specific capacitance as a function of DC bias during the measurements. Inset: the leakage current for the PSG film.

shown in the left panel of Figure 1. Next, patterned 150 nm thick IZO films were deposited on the PSG films coated glass substrate by radio-frequency (RF) magnetron sputtering with a nickel shadow mask. The sputtering was performed using an IZO ceramic target with a RF power of 100 W and a working pressure of 0.5 Pa. The size of the IZO patterns is 1000 × 150 μm. The right panel of Figure 1 illustrates the top-view image of the IZO patterns by an optical microscope (Olympus DX51). A thin IZO layer will be self-assembled between two IZO patterns with a distance of 80 μm,[27] while no IZO layer will be self-assembled between two IZO patterns with a distance of 300 μm, as schematically shown in Figure 1. When the isolated IZO pattern is deemed as the gate and the IZO patterns with self-assembled thin IZO layer are deemed as the source and drain electrodes, a laterally coupled IZO transistor is obtained. The thin IZO layer is deemed as the channel. The channel width (W) and length (L) were 1000 and 80 μm, respectively. The isolated IZO patterns were also deposited on PSG film coated ITO conductive glass substrate to obtain an IZO/PSG/ITO capacitor. Electric characteristics were performed in a probe station in air ambient with a relative humidity of ~60%. Samples were kept in a dark box to prevent interference from the visible light. Proton conductivities and frequency dependent capacitances of the PSG films were characterized by a Solartron 1260A impedance analyzer with an AC amplitude of 0.1 V and DC amplitude ranged between −0.5 and +1.0 V. Electrical performances of the laterally coupled IZO transistor were characterized by using Keithley 4200 SCS semiconductor parameter analyzer at room temperature.

3. RESULTS AND DISCUSSION

Proton conductivities (δ) of the nanogranular PSG films were measured with an IZO/PSG/ITO capacitor, as shown in the inset of Figure 2a. A typical Cole−Cole plot is shown in Figure 2a with a DC bias of 0 V. The impedance spectroscopy dada are collected as real (Re Z') and imaginary (Im Z'') components of the complex impedance. The impedance real value (R) where the impedance imaginary value is zero is used to obtain the δ value by using the following relation:

$$\delta = \frac{D}{(R - R_0)A} \quad (1)$$

chinaXiv:201703.00970v1

chinaXiv:201703.00970v1

where D, A and R_0 are the thickness of the PSG film, the electrode surface area and the resistance of electrode, respectively. The thickness D is ~1280 nm, A is ~1.5 × 10^{-3} cm^2 while R_0 is ~20 Ω. Thus, δ is estimated to be ~9.3 × 10^{-4} S/cm when DC bias is 0 V. The bias dependent δ values have also been studied, as shown in Figure 2b. It is observed that the δ values increase slightly from ~9.2 × 10^{-4} to ~9.6 × 10^{-4} S/cm with the DC bias increasing from −0.5 to +1.0 V. Frequency dependent specific capacitances of the PSG films were measured with an in-plane sandwich structure, as shown in the inset of Figure 2c. Figure 2c illustrates a typical frequency dependent specific capacitance measured with a DC bias of 0.5 V. The frequency is ranged from 1.0 Hz to 1.0 MHz. It is observed that the capacitance increases gradually with the decreased frequency. A maximum specific capacitance (C_0) of ~2.0 $\mu F/cm^2$ is obtained at 1 Hz, which is due to the formation of an EDL at the PSG/IZO interface. Under the external electric field, an oriented protons flux will be triggered within the PSG films by a sequence of proton hopping between hydroxyl groups and water molecules existed in nanogranular PSG films.[7,18] Thus, protons will accumulate at the PSG/IZO interface, resulting in a large EDL capacitance. The bias dependent EDL capacitances have also been studied, as shown in Figure 2d. It is observed that the EDL capacitance is scattered between 1.8 and 2.1 $\mu F/cm^2$ with the bias ranged between −0.5 and +1.0 V. Though the protons fluxes are triggered by the external electric field, the EDL capacitance will not be affected by the bias applied on the PSG films obviously. Thus, in the configuration of lateral coupled transistors, the bias on the lateral gate would modulate the interplay between protons and electrons at the PSG/IZO channel interface. As a result, the carrier transport characteristics of the IZO channel will be modulated, as discussed below. The inset in Figure 2d shows the leakage current of PSG films measured on the in-plane sandwich structure. A low leakage current below 5 nA is obtained in the voltage ranged from −1.5 to +1.5 V, guaranteeing that the drain current (I_{DS}) will not be affected by the leakage current.

Figure 3a shows the typical output characteristics (I_{DS} vs V_{DS}) of the laterally coupled IZO transistor. V_{DS} is scanning from 0 to 1.5 V, while V_{GS} is increased from −0.6 to +1 V in steps of 0.2 V. The output characteristics of the IZO transistor in accumulation exhibit a strong saturation and a clear pinch off. At low V_{DS}, I_{DS} increases linearly with V_{DS}, indicating that the device has a good ohmic contact. Figure 3b shows the transfer characteristics (I_{DS} vs V_{GS}) of the device with a constant V_{DS} of 1.5 V. The sweep rate is 50 mV/s. A clear anticlockwise hysteresis window (ΔV_{th}) of ~0.3 V is observed, which is likely due to the existences of mobile protons within the SiO_2 proton conductor.[28−30] The current on/off ratio is estimated to be ~5 × 10^6. The results indicate that the gate bias triggers the protons flux within the PSG layers, modulating the IZO channel conductivities obviously. A low subthreshold swing of ~110 mV/decade is observed on the laterally coupled IZO transistor. A threshold voltage (V_{th}) of ~-0.4 V is estimated from the $I_{DS}^{1/2}$ vs V_{GS} plot, indicating that the device operates in a depletion mode. Field-effect mobility (μ_{FE}) in the saturation region can be obtained by the following equation:[22]

$$I_{DS} = \frac{\mu_{FE} W C_0}{2L}(V_{GS} - V_{th})^2 \quad (2)$$

where W is channel width of 1000 μm and L is channel length of 80 μm, whereas C_0 is the EDL capacitance of ~2.0 $\mu F/cm^2$.

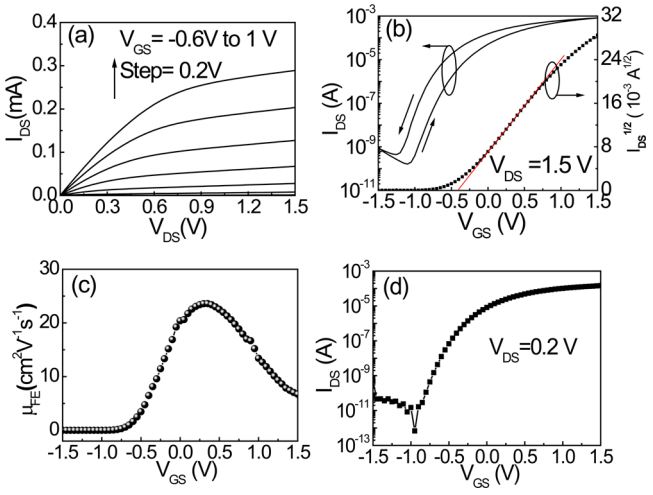

Figure 3. (a) Output curve of the laterally coupled IZO transistor. (b) Transfer curve of the laterally coupled IZO transistor measured at V_{DS} = 1.5 V. (c) Field-effect mobility (μ_{FE}) in saturation region as a function of V_{GS}. (d) Transfer characteristics of the laterally coupled IZO transistor in linear region measured at V_{DS} = 0.2 V.

The V_{GS}-dependent μ_{FE} is shown in Figure 3c. A maximum mobility of ~24 cm^2 V^{-1} s^{-1} is obtained. To investigate the interface state density (N_{it}) at the PSG/IZO channel interface, the transfer curve of the lateral coupled TFT was measured at the linear region with a fixed V_{DS} of 0.2 V, as shown in Figure 3d. The subthreshold swing (S) is estimated to be ~89 mV/decade. The interface state density (N_{it}) can be estimated by the following equation:[31]

$$N_{it} = \left(\frac{S\log(e)}{kT/q} - 1\right)\frac{C_0}{q} \quad (3)$$

where k is the Boltzmann's constant, T is the absolute temperature (300 K) and q is the electron charge. N_{it} is estimated to be ~6.1 × 10^{12} cm^{-2}, which is comparable to that for high-k oxide/semiconductor interface.[32,33]

The results discussed above indicate that the proton gating would modulate the channel conductance significantly. Transient characteristics could reflect the dynamic properties for the proton gating. Moreover, the characteristic time as an important parameter for the proton gating is also meaningful for the interfacing between electrical signals and biological response in the biological systems. Here, transient channel current induced by gate pulses through proton gating are recorded. Figure 4a shows the transient I_{DS} of the laterally coupled IZO transistor measured with a pulsed V_{GS} (1 V, 10 ms) under a constant V_{DS} of 0.2 V. At the end of the gate pulse, a peak I_{DS} of ~21.6 μA is obtained. When the gate pulse is finished, I_{DS} gradually decays back to the resting current of ~15 μA in ~500 ms. The lateral migration of protons within PSG films plays an important role for the transient I_{DS}. When a positive pulse voltage is applied on the lateral gate, protons will migrate and accumulate at the PSG/IZO channel interface, thus a high I_{DS} would be obtained, as shown in the top-left panel of Figure 4a. When the pulse voltage is finished, protons will gradually drift back to their equilibrium positions. Correspondingly, I_{DS} will decrease gradually back to the resting current. It was reported that hydrogen diffusion in a-Si, defect diffusion, oxygen vacancies diffusion and ion hopping transport in complex condensed-mater systems agreed well with a stretched

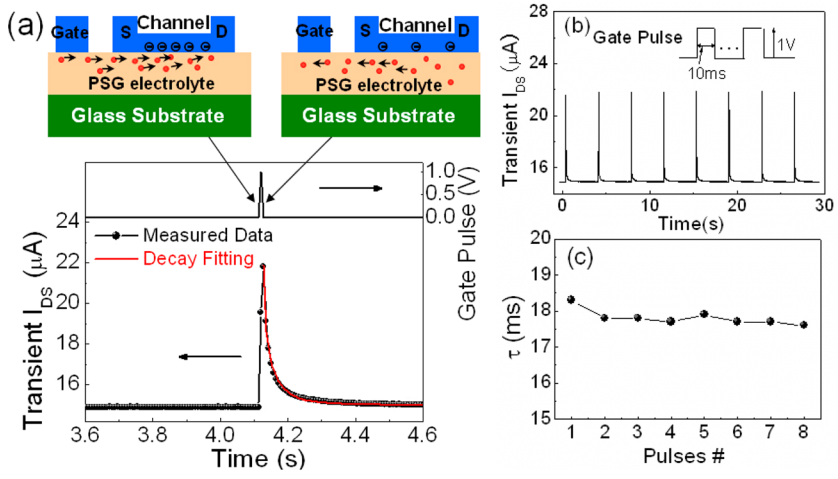

Figure 4. (a) Transient drain current of the lateral coupled IZO transistor measured with a pulsed V_{GS} (1 V, 10 ms) under a constant V_{DS} of 0.2 V. The red line illustrates that the transient I_{DS} could be fitted by stretched exponential function very well. The top panel illustrates the distributions of protons (red balls) in PSG. (b) Transient I_{DS} responses of the laterally coupled IZO transistor triggered by repeated positive gate pulses (1 V, 10 ms). (c) Retention time for transient I_{DS} in panel b.

exponential model.[34−37] Similarly, the movements of protons within nanogranular PSG films are also responsible for the decay process of I_{DS}. Thus, I_{DS} decay curves could be fitted by a stretched exponential function (SEF) shown below:[37]

$$I_{DS} = (I_0 - I_\infty)\exp\left[-\left(\frac{t - t_0}{\tau}\right)^{\beta}\right] + I_\infty \quad (4)$$

where τ is the retention time, t_0 is the time when the pulse voltage is finished, I_0 is the triggered current at the end of the pulse voltage, I_∞ is the resting current and β is the stretch index ranging between 0 and 1. A good fitting curve for the I_{DS} decay triggered by the gate pulse is obtained, as shown in Figure 4a (red line). The retention time (τ) is estimated to be ~17.8 ms. When several positive gate pulses (1 V, 10 ms) are applied on the laterally coupled IZO transistor, repeated transient I_{DS}'s are observed, as shown in Figure 4b. Each transient I_{DS} is also fitted with eq 4. The obtained τ values are shown in Figure 4c with highly stabilities.

The transient I_{DS}'s induced by negative gate pulses through proton gating are also recorded. When several negative gate pulses (−1 V, 10 ms) are applied on the laterally coupled IZO transistor, repeated transient I_{DS}'s are also observed. The transient I_{DS}'s are fitted with eq 4 too. Stable retention times (τ) of ~22 ms are obtained, as illustrated in Figure 5a. The retention time is bigger for negative gate pulses than that for positive gate pulses. Though, the slight changes, such differences can be explained as follows. The positive gate pulse will result in the accumulation of protons at the IZO channel/PSG interface. When the gate pulse ends, protons will diffuse back; the positive drain bias will promote such diffusion. Thus, the retention time is smaller. On the contrary, the negative gate pulse will result in the accumulation of protons at the gate/PSG interface. When the gate pulse ends, the positive drain bias will restrain the back diffusion of protons. Thus, the retention time is bigger. The transient I_{DS}'s are also triggered by positive pulses (1 V, 10 ms) and negative pulses (−1 V, 10 ms) in a sequential mode. The retention times for each pulse are also obtained, as shown in Figure 5b. Interestingly, the retention time is always ~18 ms for positive gate pulses and is always ~21 ms for negative gate pulses. Thus, the positive pulses and the negative pulses will not affect the transient characteristics with each other. Moreover, it could also be concluded that the intrinsic properties for proton gating will not be affected significantly by the gate pulses with the range between −1 and +1 V. The stable retention time also suggests that the proton gating is repeatable without electrochemical reaction at the interface. It is interesting to note here that the characteristic time for neural activity is several tens of milliseconds or hundreds of milliseconds,[26,38] thus the proton gated laterally coupled IZO transistors are also interesting for neuromorphic system applications.

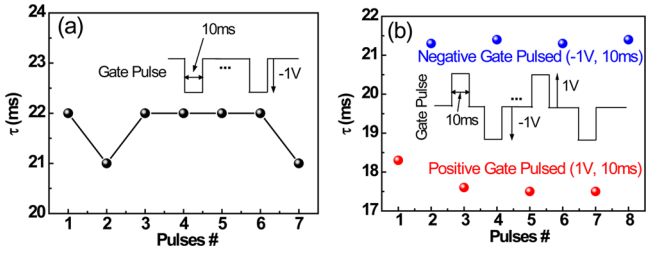

Figure 5. (a) Retention time for transient I_{DS} triggered by negative gate pulses (−1 V, 10 ms). (b) Retention time for transient I_{DS} triggered by positive and negative gate pulses in a sequential mode.

4. CONCLUSION

In summary, laterally coupled IZO transistors gated by nanogranular PSG films were fabricated on glass substrates at room temperature. Due to the modulation of the lateral protons flux within the PSG films, the IZO channel current would be modified correspondingly. Good transistor performances are obtained, including a low operation voltage of ~1.5 V, a low subthreshold swing of ~110 mV/decade, a high current on/off ratio of ~5×10^6 and a high μ_{FE} of ~24 $cm^2\ V^{-1}\ s^{-1}$. With the transient channel current triggered by gate pulses, the characteristic time for the proton gating is estimated to be ~20 ms. Due to the similar characteristic time scale between the proton gating in the laterally coupled oxide transistors and the neural activities in a biological system, the proton gated devices proposed here are interesting for portable biosensors and neuromorphic system applications.

chinaXiv:201703.00970v1

AUTHOR INFORMATION

Corresponding Author

*L. Q. Zhu. E-mail: lqzhu@nimte.ac.cn.

Notes

The authors declare no competing financial interest.

ACKNOWLEDGMENTS

This work was supported by the National Program on Key Basic Research Project (2012CB933004), the National Natural Science Foundation of China (11474293), the Zhejiang Provincial Natural Science Foundation of China (LY14A040009) and the Ningbo Natural Science Foundation (2014A610145).

REFERENCES

(1) Nam, S. W.; Rooks, M. J.; Kim, K. B.; Rossnagel, S. M. Ionic Field Effect Transistors with Sub-10 nm Multiple Nanopores. *Nano Lett.* **2009**, *9*, 2044−2048.

(2) Jiang, Z. J.; Stein, D. Charge Regulation in Nanopore Ionic Field-Effect Transistors. *Phys. Rev. E* **2011**, *83*, 031203.

(3) Matovic, J.; Adamovic, N.; Radovanovic, F.; Jaksic, Z.; Schmid, U. Field Effect Transistor Based on Ions as Charge Carriers. *Sens. Actuators, B* **2012**, *170*, 137−142.

(4) Tybrandt, K.; Forchheimer, R.; Bergren, M. Logic Gates Based on Ion Transistors. *Nat. Commun.* **2012**, *3*, 871.

(5) Hou, X.; Guo, W.; Jiang, L. Biomimetic Smart Nanopores and Nanochannels. *Chem. Soc. Rev.* **2011**, *40*, 2385−2401.

(6) Joshi, P.; Smolyanitsky, A.; Petrossian, L.; Goryll, M.; Saraniti, M.; Thornton, T. J. Field Effect Modulation of Ionic Conductance of Cylindrical Silicon-on-Insulator Nanopore Array. *J. Appl. Phys.* **2010**, *107*, 054701.

(7) Zhong, C.; Deng, Y.; Roudsari, A. F.; Kapetanovic, A.; Anantram, M. P.; Rolandi, M. A Polysaccharide Bioprotonic Field-Effect Transistor. *Nat. Commun.* **2011**, *2*, 476.

(8) Ueno, K.; Nakamura, S.; Shimotani, H.; Ohtomo, A.; Kimura, N.; Nojima, T.; Aoki, H.; Iwasa, Y.; Kawasaki, M. Electric-Field-Induced Superconductivity in an Insulator. *Nat. Mater.* **2008**, *7*, 855−858.

(9) Larsson, O.; Said, E.; Berggren, M.; Crispin, X. Insulator Polarization Mechanisms in Polyelectrolyte-Gated Organic Field-Effect Transistors. *Adv. Funct. Mater.* **2009**, *19*, 3334−3341.

(10) Yuan, H. T.; Shimotani, H.; Ye, J. T.; Yoon, S.; Aliah, H.; Tsukazaki, A.; Kawasaki, M.; Iwasa, Y. Electrostatic and Electrochemical Nature of Liquid-Gated Electric-Double-Layer Transistors Based on Oxide Semiconductors. *J. Am. Chem. Soc.* **2010**, *132*, 18402−18407.

(11) Kim, S. H.; Hong, K.; Xie, W.; Lee, K. H.; Zhang, S.; Lodge, T. P.; Frisbie, C. D. Electrolyte-Gated Transistors for Organic and Printed Electronics. *Adv. Mater.* **2013**, *25*, 1822−1846.

(12) Ye, J. T.; Inoue, S.; Kobayashi, K.; Kasahara, Y.; Yuan, H. T.; Shimotani, H.; Iwasa, Y. Liquid-Gated Interface Superconductivity on an Atomically Flat Film. *Nat. Mater.* **2010**, *9*, 125−128.

(13) Wu, P. H.; Ishii, S.; Tanabe, K.; Munakata, K.; Hammond, R. H.; Tokiwa, K.; Geballe, T. H.; Beasley, M. R. Synthesis and Ionic Liquid Gating of Hexagonal WO_3 Thin Films. *Appl. Phys. Lett.* **2015**, *106*, 042602.

(14) Shimizu, S.; Takahashi, K. S.; Kubota, M.; Kawasaki, M.; Tokura, Y.; Iwasa, Y. Gate Tuning of Anomalous Hall Effect in Ferromagnetic Metal $SrRuO_3$. *Appl. Phys. Lett.* **2014**, *105*, 163509.

(15) Jiang, J.; Wan, Q.; Sun, J.; Lu, A. X. Ultralow-Voltage Transparent Electric-Double-Layer Thin-Film Transistors Processed at Room-Temperature. *Appl. Phys. Lett.* **2009**, *95*, 152114.

(16) Jiang, J.; Sun, J.; Zhou, B.; Lu, A. X.; Wan, Q. Self-Assembled in-Plane Gate Oxide-Based Homojunction Thin-Film Transistors. *IEEE Electron Device Lett.* **2011**, *32*, 500−502.

(17) Sun, J.; Jiang, J.; Dou, W.; Zhou, B.; Wan, Q. Anomalous Threshold Voltage Shift and Surface Passivation of Transparent Indium-Zinc-Oxide Electric-Double-Layer TFTs. *Lett.* **2011**, *32*, 910−912.

(18) Zhu, L. Q.; Sun, J.; Wu, G. D.; Zhang, H. L.; Wan, Q. Self-Assembled Dual in-Plane Gate Thin-Film Transistors Gated by Nanogranular SiO_2 Proton Conductors for Logic Applications. *Nanoscale* **2013**, *5*, 1980−1985.

(19) Zhang, H. L.; Guo, L. Q.; Wan, Q. Nanogranular Al_2O_3 Proton Conducting Films for Low-Voltage Oxide-based Homojunction Thin-Film Transistors. *J. Mater. Chem. C* **2013**, *1*, 2781−2786.

(20) Zhang, H. L.; Wan, Q.; Wan, C. J.; Wu, G. D.; Zhu, L. Q. Tungsten Oxide Proton Conducting Films for Low-Voltage Transparent Oxide-based Thin-Film Transistors. *Appl. Phys. Lett.* **2013**, *102*, 052905.

(21) Zhu, D. M.; Men, C. L.; Wan, X.; Deng, C.; Li, Z. P. Self-Assembled In-Plane-Gate Thin-Film Transistors Gated by WO_x Solid-State Electrolytes. *Chin. Phys. Lett.* **2013**, *30*, 087302.

(22) Zhou, B.; Sun, J.; Han, X.; Jiang, J.; Wan, Q. Low-Voltage Organic/Inorganic Hybrid Transparent Thin-Film Transistors Gated by Chitosan-based Proton Conductors. *IEEE Electron Device Lett.* **2011**, *32*, 1549−1551.

(23) Dou, W.; Jiang, J.; Sun, J.; Zhou, B.; Wan, Q. Low-Voltage Oxide-based Electric-Double-Layer TFTs Gated by Stacked SiO_2 Electrolyte/Chitosan Hybrid Dielectrics. *IEEE Electron Device Lett.* **2012**, *33*, 848−850.

(24) Wu, G. D.; Zhang, J.; Wan, X.; Yang, Y.; Jiang, S. H. Chitosan-based Biopolysaccharide Proton Conductors for Synaptic Transistors on Paper Substrates. *J. Mater. Chem. C* **2014**, *2*, 6249−6255.

(25) Voglis, G.; Tavernarakis, N. The Role of Synaptic Ion Channels in Synaptic Plasticity. *EMBO Rep.* **2006**, *7*, 1104−1110.

(26) Mukhamedyarov, M. A.; Grishin, S. N.; Zefirov, A. L.; Palotas, A. The Mechanisms of Multi-component Paired-Pulse Facilitation of Neurotransmitter Release at the Frog Neuromuscular Junction. *Pfluegers Arch.* **2009**, *458*, 563−570.

(27) Lu, A. X.; Sun, J.; Jiang, J.; Wan, Q. One-Shadow-Mask Self-Assembled Ultralow-Voltage Coplanar Homojunction Thin-Film Transistors. *IEEE Electron Device Lett.* **2010**, *31*, 1137−1139.

(28) Lu, A. X.; Sun, J.; Jiang, J.; Wan, Q. Low-Voltage Transparent Electric-Double-Layer ZnO-based Thin-Film Transistors for Portable Transparent Electronics. *Appl. Phys. Lett.* **2010**, *96*, 043114.

(29) Zhu, L. Q.; Chao, J. Y.; Xiao, H. Lateral Protonic/Electronic Hybrid Oxide Thin-Film Transistor Gated by SiO_2 Nanogranular Films. *Appl. Phys. Lett.* **2014**, *105*, 243508.

(30) Yuan, H. T.; Shimotani, H.; Tsukazaki, A.; Ohtomo, A.; Kawasaki, M.; Iwasa, Y. Hydrogenation-Induced Surface Polarity Recognition and Proton Memory Behavior at Protic-Ionic-Liquid/Oxide Electric-Double-Layer Interfaces. *J. Am. Chem. Soc.* **2010**, *132*, 6672−6678.

(31) Choi, H.-S.; Jeon, S.; Kim, H.; Shin, J.; Kim, C.; Chung, U.-I. Verification of Interface State Properties of a-InGaZnO Thin-Film Transistors With SiN_x and SiO_2 Gate Dielectrics by Low-Frequency Noise Measurements. *IEEE Electron Device Lett.* **2011**, *32*, 1083−1085.

(32) Zhang, L.; Li, J.; Zhang, X. W.; Jiang, X. Y.; Zhang, Z. L. High Performance ZnO-Thin-Film Transistor with Ta_2O_5 Dielectrics Fabricated at Room Temperature. *Appl. Phys. Lett.* **2009**, *95*, 072112.

(33) Martins, R.; Barquinha, P.; Ferreira, I.; Pereira, L.; Gonçalves, G.; Fortunato, E. J. Role of Order and Disorder on the Electronic Performances of Oxide Semiconductor Thin Film Transistors. *J. Appl. Phys.* **2007**, *101*, 044505.

(34) Chang, T.; Jo, S. H.; Lu, W. Short-Term Memory to Long-Term Memory Transition in a Nanoscale Memristor. *ACS Nano* **2011**, *5*, 7669−7676.

(35) Wang, Z. Q.; Xu, H. Y.; Li, X. H.; Yu, H.; Liu, Y. C.; Zhu, X. J. Synaptic Learning and Memory Functions Achieved Using Oxygen Ion Migration/Diffusion in an Amorphous InGaZnO Memristor. *Adv. Funct. Mater.* **2012**, *22*, 2759−2765.

(36) Kakalios, J.; Street, R. A.; Jackson, W. B. Stretched-Exponential Relaxation Arising from Dispersive Diffusion of Hydrogen Amorphous-Silicon. *Phys. Rev. Lett.* **1987**, *59*, 1037−1040.

chinaXiv:201703.00970v1

(37) Sturman, B.; Podivilov, E. Origin of Stretched Exponential Relaxation for Hopping-Transport Models. *Phys. Rev. Lett.* **2003**, *91*, 176602.
(38) Zucker, R. S.; Regehr, W. G. Short-Term Synaptic Plasticity. *Annu. Rev. Physiol.* **2002**, *64*, 355–405.

chinaXiv:201703.00970v1